IEEE Access
Multidisciplinary ⋮ Rapid Review ⋮ Open Access Journal

Received 8 March 2023, accepted 5 April 2023, date of publication 7 April 2023, date of current version 12 April 2023.

Digital Object Identifier 10.1109/ACCESS.2023.3265563

RESEARCH ARTICLE

Evaluating the Effectiveness of Planar and Waveguide 3D-Printed Antennas Manufactured Using Dielectric and Conductive Filaments

RICCARDO COLELLA[1], (Senior Member, IEEE), FRANCESCO P. CHIETERA[1], (Student Member, IEEE), GIACOMO MUNTONI[2], GIOVANNI A. CASULA[2], (Senior Member, IEEE), GIORGIO MONTISCI[2], (Senior Member, IEEE), AND LUCA CATARINUCCI[1], (Senior Member, IEEE)

[1]Department of Engineering for Innovation, University of Salento, 73100 Lecce, Italy
[2]Dipartimento di Ingegneria Elettrica ed Elettronica, Università degli Studi di Cagliari, 09123 Cagliari, Italy

Corresponding author: Giorgio Montisci (giorgio.montisci@unica.it)

ABSTRACT 3D printing is a technology suitable for creating electronics and electromagnetic devices. However, the manufacturing of both dielectric and conductive parts in the same process still remain a challenging task. This study explores the combination of 3D printing with traditional manufacturing techniques for antenna design and fabrication, giving the designer the advantage of using the additive manufacturing technology only to implement the most critical parts of a certain structure, ensuring a satisfying electromagnetic performance, but limiting the production cost and complexity. In the former part of the study, the focus is on three proximity-coupled patch antennas. It demonstrates how hybrid devices made of metal, dielectric, and 3D-printed (using Fused Filament Fabrication) conductive polymers can be successfully simulated and created for different operating frequency bands. In the latter part, the study compares three prototypes of a 5G-NR, high gain, and wideband waveguide antenna: respectively a fully 3D printed one made of electrifi (which is the most conductive commercial 3D-printable filament), an all-metal one, and a hybrid (3D-printed electrifi & metal) one. The results show a 15% reduction in efficiency when using the all-Electrifi configuration compared to all-metal one, and a 4-5% reduction when using the hybrid version.

INDEX TERMS Additive manufacturing, conductive filaments, fused filament fabrication, patch antennas, waveguide antennas, 3D-printed antennas.

I. INTRODUCTION

3D printing technologies are progressively transforming traditional production and prototyping methods thanks to their ease, speed, low cost and sustainability, with benefits also in the fields of RF electronics and electromagnetics. The accuracy of next-generation printers and the expanding range of printable materials enable the design and production of increasingly complex structures that would otherwise be difficult or costly to produce using conventional techniques [1], [2], [3], [4].

The associate editor coordinating the review of this manuscript and approving it for publication was Ali Karami Horestani.

Among the various 3D printing technologies that can be used by antenna designers to realize arbitrarily complex antenna structures, the most used are Material Jetting, Binder Jetting, Laser Powder Bed Fusion, Directed Energy Deposition, Sheet Lamination, Vat Photopolymerization, and Fused Filament Fabrication (FFF) [5], [6], [7], [8]. The choice of a specific technique mainly depends on materials, design precision, working frequency, and overall cost.

For sub-6 GHz applications, FFF technique is a good choice because it guarantees the right mix of affordability and simplicity, with a more than satisfactory resolution. Conversely, when the frequency increases, or when an higher precision level is required by the design, alternatives to FFF

are either the – expensive – 3D metal printing [9] or the binder jetting, which can achieve higher resolutions, but with the need for high temperature sintering to get the desired electrical conductivity [10]. This is the main reason why in the open literature only a few fully 3D printed antennas have been presented, so far.

Consequently, FFF-based techniques, or other 3D-printing methods based on material extrusion, are mainly used in the literature to manufacture the dielectric structure/support of the antenna, resorting to alternative solutions to suitably create its conductive parts [11], [12], [13], [14], [15], [16], [17], [18], [19], [20], [21], [22], [23], [24], [25], [26]. Specifically, four main approaches can be used:

1) conductive tape (usually copper or aluminum) [11], [12], [13];
2) conductive paint (or similarly spray coating or conductive ink) [13], [14], [15], [16], [17], [18], [19];
3) galvanic plating [5], [13], [20], [21], [22], [23], [24];
4) conductive filament [13], [25], [26].

The primary drawback of the first three methods is their two-step approach: they involve 3D printing the supportive/dielectric structure first, then incorporating the conductive component through a separate technique, leading to increased complexity and higher production costs. Conversely, approach 4) presents a more desirable solution with a single, unified 3D-Printing production process leveraging on both dielectric and conductive filaments.

As for these lasts, among the several filaments available on the market composed of a blend of polymers and a certain percentage of conductive parts (graphene in the Black-Magic filament [27], conductive black carbon in the Proto-Pasta filament [28], carbon nanotubes in the Fiberforce Conductive filament [29], copper in the Electrifi filament [30]), Electrifi is the most promising one. Several researchers investigated its properties recently and used it to implement 3D Printed antennas and microwave devices [6], [25], [31], including fully 3D-printed antennas [6], [13], [25], [32], based on Electrifi and PLA.

A thorough electromagnetic characterization of Multi3D Electrifi filament conductivity has been carried out in [33] across a wide frequency range (0.72 to 6 GHz), taking into account both the deposition of the conductive polymer on a printed PLA substrate and the roughness of the substrate and conductive parts. This characterization has been verified using fully 3D-printed monopole antennas covering the entire frequency range, confirming that Electrifi is a suitable material for designing 3D printed antennas up to 6 GHz.

Despite its suitability to realize RF devices, the electrical conductivity of Electrifi is several orders of magnitude lower than bulk metals, thus affecting the overall antenna performance. In this regard, it could be useful to investigate if Electrifi can only be used for the fabrication of those conductive parts that benefit from complex geometries, paired with parts made through traditional manufacturing techniques where standard shapes can be used.

In this work, such "hybrid" designs are studied, presenting radiating structures realized combining 3D-printed and conventionally manufactured parts. More in detail, two antenna topologies have been selected for this scope:

1) three different proximity-coupled patch antenna configurations based on the same layout, where only the patch has been implemented in Electrifi to focus on the achievable radiating efficiency and electromagnetic performance. They have been designed at three different frequencies within the band validated in [33] so exploiting the available electrical conductivity of the Electrifi;
2) a waveguide antenna working from 3.3 GHz to 3.8 GHz for 5G-NR band applications, with an improved bandwidth and gain achieved by exploiting the free-form advantages enabled by Additive Manufacturing (AM). In this case, three different prototypes have been fabricated and compared, consisting of Electrifi only, purely metallic, and a combination of 3D-printed Electrifi parts and standard metallic parts.

These hybrid solutions give the designer the considerable advantage of using the AM only to implement the most critical parts of a certain structure, ensuring a satisfying electromagnetic behavior of the device, but considerably limiting the production cost and complexity.

II. 3D PRINTED PROXIMITY COUPLED PACTH ANTENNAS

The first configuration employed to investigate the potentiality of a hybrid solution is a 5-layer proximity coupled microstrip patch antenna (PCPA). The antenna substrates are manufactured using 3D-printed PLA, with dielectric permittivity 2.5 and loss tangent between 0.01 and 0.02 in the frequency range of interest [33]. The ground plane is made of copper, and the feeding microstrip is realized using a 35 μm-copper tape. Finally, the radiating patch, i.e., the component best suited to take advantage of the free-form capabilities offered by 3D printing technology, was fabricated using the Electrifi conductive filament. For the sake of simplicity, but without loss of generality, in this work we have used a simple planar rectangular patch (see Fig. 1). However, using a conductive filament for the radiating patch can facilitate the

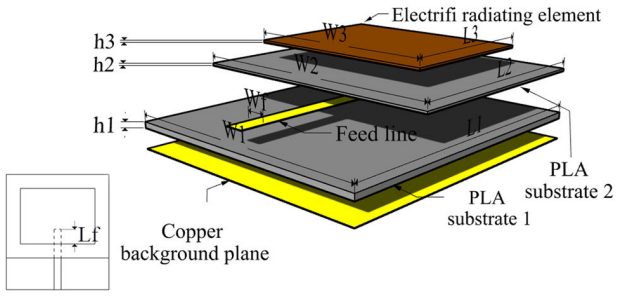

FIGURE 1. Exploded view of a generic proximity coupled patch antenna model.

manufacturing of more complex geometries exploiting also the third dimension (see e.g. [34], [35]).

Since the conductivity of the 3D-printed Electrifi filament depends on the frequency, as reported in [33] up to 6 GHz, three prototypes of the proximity coupled patch antenna have been manufactured, resonating at 2.5 GHz, 4.1 GHz, and 5 GHz. According to the characterization provided in [33], the corresponding values of the Electrifi conductivity, set in the design procedures, are 2800 S/m at 2.5 GHz, 3100 S/m at 4.1 GHz, and 3650 S/m at 5 GHz. CST Studio Suite has been used for the design and simulations. The geometrical parameters of the designed antenna are reported in Table 1.

TABLE 1. Geometrical parameters of the designed PCPAs.

	2.5 GHz	4.1 GHz	5 GHz
h1 (mm)	1.47	1.47	1.47
h2 (mm)	0.57	0.57	0.57
W1 (mm)	64.6	64.6	64.6
L1 (mm)	72.6	72.6	72.6
W2 (mm)	64.6	64.6	64.6
L2 (mm)	56.8	57.28	56.8
W3 (mm)	47	16.3	23
L3 (mm)	35	22.97	16.3
Wf (mm)	4.4	4.4	4.4
Lf (mm)	9.2	7.88	4.2
H3 (mm)	0.6	0.6	0.6

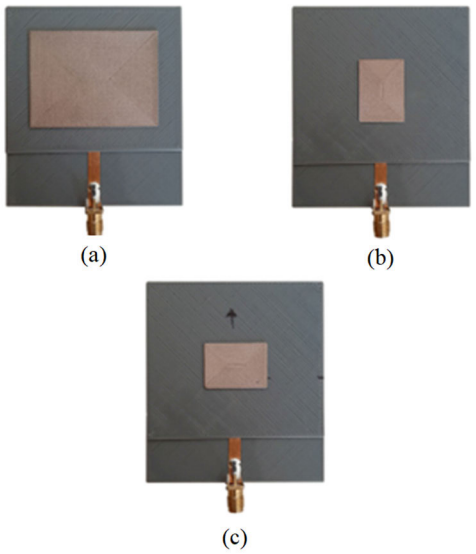

FIGURE 2. Photo of the manufactured prototypes of the PCPAs designed to operate at 2.5 GHz (a), 4.1 GHz (b), and 5 GHz (c), respectively.

Prototypes of these antennas have been manufactured and measured in the EMTech laboratory of the Department of Engineering for Innovation of the University of Salento (see Fig. 2). The commercial 3D printer CREALITY CR20 PRO has been used. The layer thickness has been set to 0.3 mm with a 100% infill. An aligned rectilinear pattern

TABLE 2. 3D printing setting parameters.

Material	Extruding Temp. (°C)	Printing Speed (mm/min)	Nozzle Diameter (mm)	Extrusion Multiplier (%)
PLA	205 °C	2600	0.5	100
Electrifi	145 °C	600	0.5	120

(with 90° cross hatching) has been used for the PLA substrates, while a concentrical pattern has been used for the radiating parts. The other printing parameters as reported in Table 2.

In Fig. 3 the reflection coefficient of the manufactured prototypes is depicted with a very good agreement between simulations and measurement.

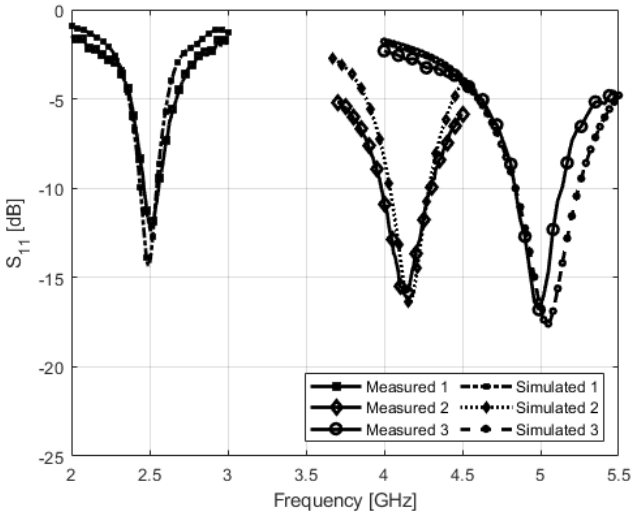

FIGURE 3. Comparison between simulated and measured S_{11} of the three proximity coupled patch antennas.

In Table 3 the simulated electromagnetic performance of the three PCPAs is reported, showing also the comparison with the same antennas simulated using a copper patch instead of the one made of Electrifi. The copper patches exhibit a higher efficiency if compared with the ones realized with the Electrifi filament and, as expected, the efficiency gap is higher for lower frequencies and decreases when the frequency increases, because of the corresponding increment

TABLE 3. Electromagnetic performance comparison of the designed proximity coupled patch antennas.

	Prototype @ 2.5 GHz		Prototype @ 4.1 GHz		Prototype @ 5 GHz	
	Electrifi	Copper	Electrifi	Copper	Electrifi	Copper
G_R (dBi)	2.3	5.3	3.4	5.2	5.3	5.4
D (dBi)	7.1	7.3	7.45	6.2	8	6.5
η (%)	33	63	39	78	54	83

of the Electrifi conductivity (from 2800 S/m at 2.5 GHz to 3650 S/m at 5 GHz) [33].

III. FULLY 3D-PRINTED WIDEBAND ANTENNA FOR 3.3-3.8 GHZ 5G APPLICATIONS

The second antenna configuration selected to investigate the effectiveness of the Electrifi in more complex manufacturing contexts, is a circular waveguide antenna with relatively high gain (higher than 8 dBi) in 5G NR (New Radio) Band N78 (3300-3800 MHz), which is the most used 5G band in Europe [36].

Starting with a very common narrowband circular waveguide antenna, whose schematic is reported in Fig. 4, the free-form factor enabled by additive manufacturing 3D-printing is exploited to "model" and adjust the antenna shape aiming to a higher bandwidth and the desired gain.

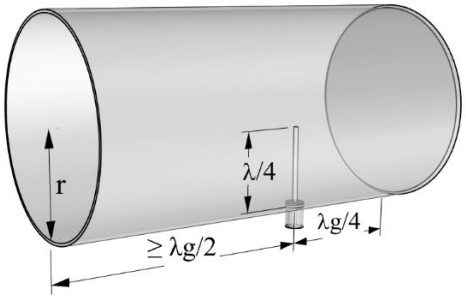

FIGURE 4. Structure of a canonical narrowband and gain-limited circular waveguide antenna.

More specifically, the basic principle of the canonical circular waveguide antenna of Fig. 4 consists of feeding the antenna with a $\lambda/4$ monopole placed at $\lambda_g/4$ (where λ_g is the guide wavelength) from the metal background to guarantee an in-phase sum of the contributions. The radius of the circular waveguide is chosen large enough to assure the propagation of the TE_{11} mode at the desired frequency, and not the TM_{01} mode. The well-known formulas for the cutoff frequencies of the two aforementioned modes are reported below along with the guide wavelength λ_g associated to the fundamental mode TE_{11} [37]:

$$f_{c-TE_{11}} = 1.841 \cdot c/2\pi r \quad (1)$$

$$f_{c-TM_{01}} = 2.405 \cdot c/2\pi r \quad (2)$$

$$\lambda_g = 2\pi/\beta \quad (3)$$

Moreover, the useful although approximated formula which links the maximum directivity of an antenna with its maximum effective aperture A_{em} is also reported [38]:

$$D = \left(4\pi/\lambda^2\right) \cdot A_{em} \quad (4)$$

The distance between aperture and monopole must be higher than $\lambda_g/2$ so to have all the higher-order modes completely suppressed and the TE_{11} mode well formed. Consequently, the minimum length of the antenna becomes $3\lambda_g/4$. For instance, for a targeted working frequency of 3.6 GHz, a radius of 2.7 cm could be considered, resulting in a f_{c-TE11} of 3.25 GHz and a f_{c-TM01} of 4.25 GHz. The related λ_g results 19.5 cm and hence the total length of the antenna around 14.6 cm. Finally, the length of the monopole results $\lambda/4 = 2.08$ cm, whilst the expected maximum directivity $D = 6.17$ dBi at a frequency of 3.6 GHz, according to (4) where effective aperture is approximated with the physical one. Moreover, an antenna designed this way, has typically a narrow-band behavior, inherited by that of the simple monopole used to feed the structure. The circular waveguide antenna is generally quite attractive since both circular metallic structures and wire-monopoles can be realized with cost-effective fabrication processes. Nevertheless, when the radiating element and the guiding structure lose their regularity, advantages from the electromagnetic point of view can be obtained but at the expense of an ad-hoc and more complex manufacturing process.

To verify whether the direct 3D-printing of conductive parts can fill this gap, in Fig. 5, a new modified version of the same antenna is proposed. It is designed to increase bandwidth and gain by acting on the shape of both the radiating element and the guiding structure. In particular, the filiform monopole is replaced by a bow-tie inspired triangular-shaped monopolar structure whose dimensions (s, h, and θ in Fig. 5) must be optimized to obtain the desired band and input impedance. Furthermore, the higher gain is ensured by a horn termination which smoothly expands the effective area of the antenna and consequently its directivity and gain.

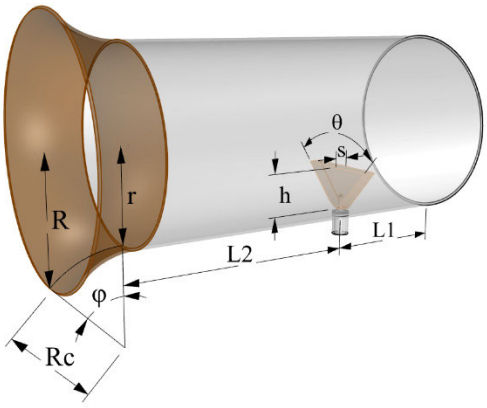

FIGURE 5. Schematic structure for a modified wider-band and higher gain circular waveguide antenna.

Without loss of generality, for the specific case of a 3.3-3.8 GHz 5G band, the waveguide inner radius has been set at 2.97 cm, in order to have the cutoff frequency of the TE_{11} mode at 2.95 GHz (through (1)). In this way, the rule of thumb which suggests having the lowest working frequency (i.e. 3.3 GHz) at least 10% higher than the cutoff frequency of the fundamental mode is respected. This is also necessary to avoid a too large λ_g which would cause a large-sized antenna. Again, the cutoff frequency of the first higher-order mode

resulting from (2) is $f_{c-TM01} = 3.86$ GHz, which is larger than the highest desired working frequency, i.e., 3.8 GHz.

Moreover, to assure a minimum gain of 8 dBi, in this specific example, the maximum radius of the horn has been set at a value of $R = 3.92$ cm (see Fig. 5), from which we can estimate through (4) a directivity value around 8.65 dBi at 3.3 GHz, 9.29 dBi at 3.55 GHz, and 9.88 dBi at 3.8 GHz. For sake of simplicity, the physical aperture has been used in the formula, instead of the effective one. Having the possibility of arbitrary shaping the horn termination, a filleted profile (defined by an arc of circumference of radius Rc and angle φ as shown in Fig. 5) instead of a chamfered one has been chosen for the antenna aperture. This allows to have a smoother transition with the circular waveguide.

The structure has been simulated through CST Studio Suite by using the conductivity value obtained in [33] for the range 3.0 - 4.5 GHz, which corresponds to $\sigma = 3100$ S/m. The parameters of Fig. 5 have been tuned so to obtain the desired bandwidth and gain. Results are summarized in Table 4.

TABLE 4. Dimensions for the Electrifi-made waveguide antenna.

Parameter	Dimension
r	29.7 mm
R	39.2 mm
L1	41 mm
L2	73.2 mm
h	14 mm
s	4 mm
Rc	30 mm
θ	85 degrees
φ	45 degrees

The models of both the main structure and the bow-tie inspired monopole have been 3D-printed in Electrifi. Due to the relevant size of the structure, a 0.5 mm-thick extruder and a layer height of 0.3 mm have been used so to make

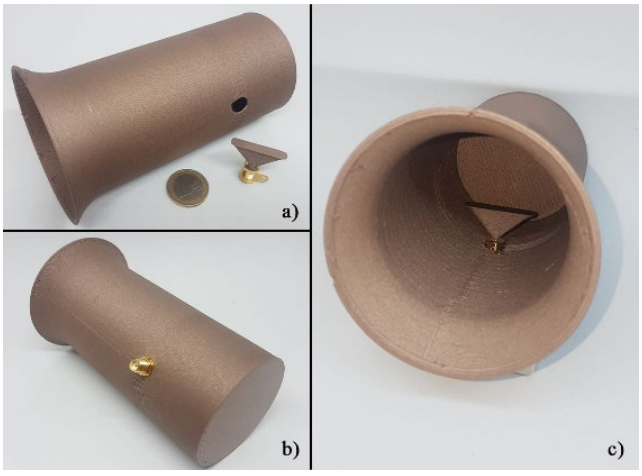

FIGURE 6. Different view of the fully-3D-printed circular waveguide antenna: unmounted (a), assembled, external view (b), assembled, inner view (c).

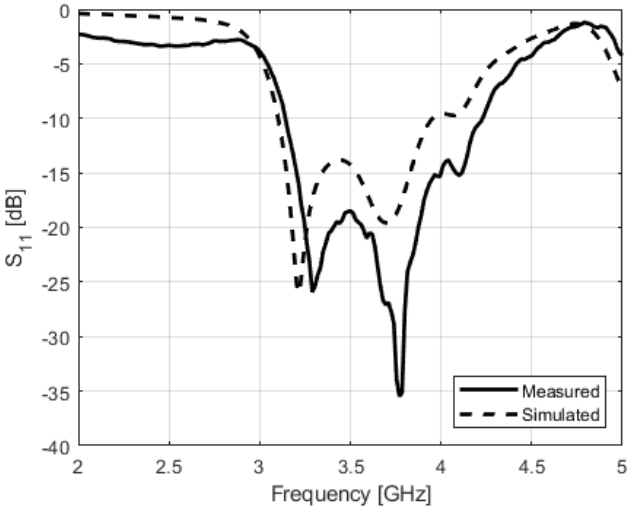

FIGURE 7. Comparison between simulated and measured S_{11} curves for the Electrifi made waveguide antenna.

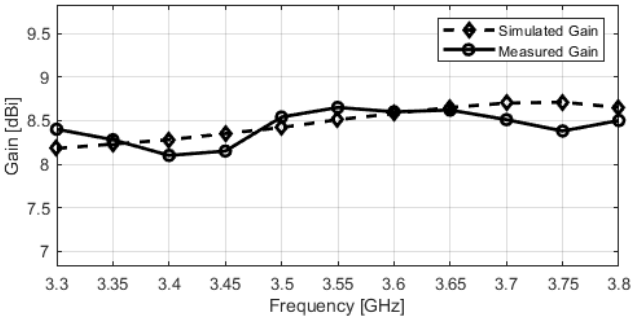

FIGURE 8. Comparison between simulated and measured gain of the Electrifi made waveguide antenna.

the printing process faster as well as strengthen the printed pieces. A temperature of 60 °C has been set on the heated bed of the printer in order to ensure a better adhesion of the whole structure during the barely four hours of printing. Once printed, the whole antenna has been straightforwardly assembled by means of an SMA connector. The final result is reported in Fig. 6 along with details of the printed elements. It is worth highlighting how this prototype realization represents a severe test for the use of additive manufacturing by FFF 3D-printing in antenna devices production. This is due to the relatively large size of the main model as well as to the specific characteristic of the printing filament, which needs a skillful approach to be successfully printed.

In Fig. 7, the comparison between simulated and measured S_{11} scattering parameters is reported, and a very good agreement can be observed, thus demonstrating once again that the electromagnetic characterization of printed Electrifi filaments is rather effective. Moreover, it is clear how the implementation of a customized bow-tie inspired monopole to feed the structure has determined a significant wide band behavior of the final antenna, with a return loss below -10 dB in a band even wider of the desired one.

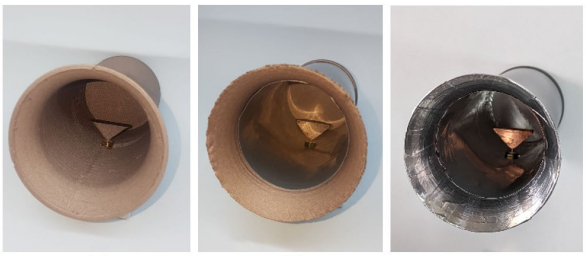

FIGURE 9. Visual comparison of the three realized models. Respectively Fully 3D-printed (a), Hybrid (b), and Metal-lined (c).

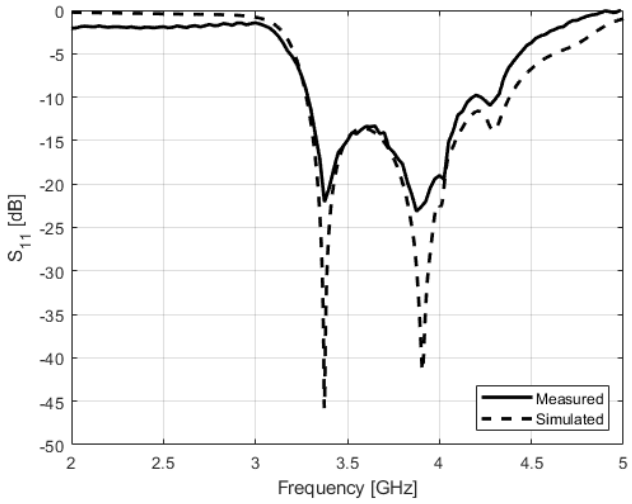

(a)

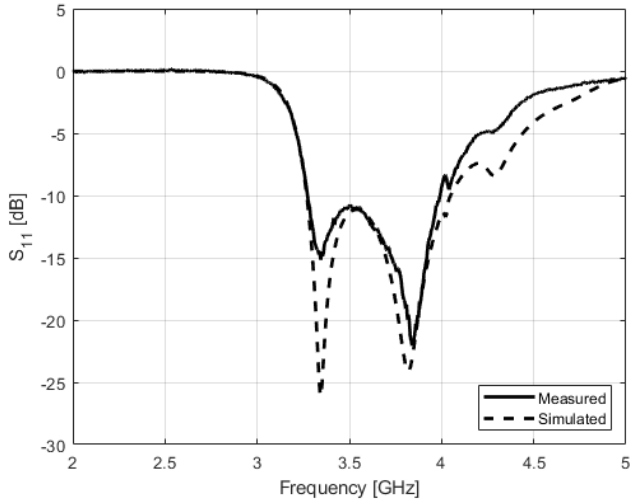

(b)

FIGURE 10. Comparison between simulated and measured S_{11} curves for the hybrid (a) and metal-lined (b) antennas.

In Fig. 8, the comparison between simulated and measured gain over frequency has also been reported. As can be appreciated, there is a good agreement among the two curves, even if the measured one is slightly higher than the simulated one

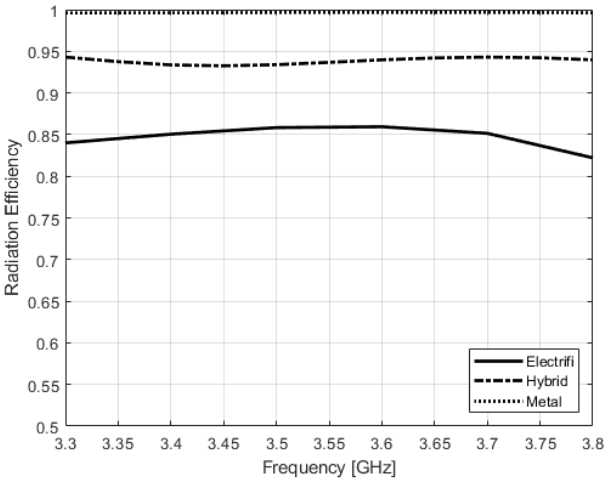

FIGURE 11. Visual comparison of the simulated radiation efficiency. Respectively for the fully 3D-printed (a), hybrid (b), and metal-lined (c) antennas.

for the whole set of measurement points. As for the radiation efficiency, it ranges from -0.64 dB at 3.55 GHz, and -0.78 dB at 3.8 GHz.

IV. CONSIDERATIONS ON AN HYBRID APPROACH IN DESIGNING ELECTROMAGNETIC DEVICES

The previous section shows that 3D printing can be effectively used to design and manufacture performing electromagnetic devices that exploit unconventional shapes. However, a different and cost-effective approach can be followed, which consists of combining complex parts that greatly benefit from additive manufacturing (such as the bow-tie-inspired monopole and horn), with more standard parts that can be inexpensively and easily produced (such as the cylindrical central body). Specifically, a cylindrical waveguide antenna operating in the same frequency band, has been designed and created by combining 3D-printed elements with metallic parts made through simple industrial productions. Moreover, a third full-metal waveguide antenna has been designed and realized to evaluate the impact of the polymeric conductive material on the performance of the bow-tie monopole and horn aperture.

A visual comparison of the three realized prototypes is reported in Fig. 9.

The good agreement between simulations and measurements in terms of S_{11} curves can be appreciated in Fig. 10 for the hybrid (a) and fully metal (b) prototypes.

Finally, in Fig. 11, the comparison among the simulated radiation efficiency of the three antennas is shown.

The fully 3D-printed antenna exhibits the lower efficiency, and this is not surprising, although its value is around 85%, which is remarkable considering that the antenna is fully Electrifi made. For the hybrid antenna, with the cylinder made with metal, the efficiency increases up to 94%, and rises to barely 99% when also the feeding monopole is realized with copper.

We can conclude that the hybrid approach of combining 3D-printed and conventionally manufactured parts in electromagnetic device design is a viable option. This method leverages the benefits of AM in creating unique and advantageous shapes with different materials and techniques, while minimizing conductivity limitations of available filaments by incorporating conventional metallic parts for traditional shapes.

V. CONCLUSION

3D-printable conductive filaments are captivating and promise applications in various fields, including electromagnetics. However, the relatively lower electrical conductivity than bulk metals impacts performance. In this study, based on previous work by the authors on the electromagnetic characterization of a 3D-printable conductive filament (Electrifi), new categories of 3D-printed antennas have been studied. These are hybrid antennas, combining parts produced with conventional techniques with 3D-printed parts where the free-form-factor is essential.

We focused on two antenna topologies, namely different narrowband proximity-coupled patch antennas and a circular waveguide antenna with a broadband bow-tie monopole feed. The latter has been made in three different versions: fully in Electrifi to demonstrate full 3D-printability, completely in aluminum as a reference, and hybrid, with the circular guide in aluminum and the feeder and horn in Electrifi.

In all tested cases we obtained a very good agreement between simulated and measured data, both in terms of reflection coefficient and efficiency. The fully Electrifi-made prototype experiments a 15% reduction in efficiency if compared with a fully metal prototype, while a hybrid prototype shows a decrement of only 4-5%. Therefore, the hybrid approach is a viable option leveraging the benefits of AM in creating arbitrarily complex shapes, but minimizing the degradation of the performance due to the low conductivity of available filaments by implementing the traditional shapes using conventional metallic parts. This solution ensures a good electromagnetic behavior of the designed structure, significantly lowering both the production cost and complexity.

REFERENCES

[1] M. Vaezi, H. Seitz, and S. Yang, "A review on 3D micro-additive manufacturing technologies," *Int. J. Adv. Manuf. Technol.*, vol. 67, nos. 5–8, pp. 1721–1754, Jul. 2013.

[2] E. MacDonald, R. Salas, D. Espalin, M. Perez, E. Aguilera, D. Muse, and R. B. Wicker, "3D printing for the rapid prototyping of structural electronics," *IEEE Access*, vol. 2, pp. 234–242, 2014.

[3] C. Kim, D. Espalin, M. Liang, H. Xin, A. Cuaron, I. Varela, E. Macdonald, and R. B. Wicker, "3D printed electronics with high performance, multilayered electrical interconnect," *IEEE Access*, vol. 5, pp. 25286–25294, 2017.

[4] A. Georgiadis, J. Kimionis, and M. M. Tentzeris, "3D/inkjet-printed millimeter wave components and interconnects for communication and sensing," in *Proc. IEEE Compound Semiconductor Integr. Circuit Symp. (CSICS)*, Miami, FL, USA, Oct. 2017, pp. 1–4.

[5] K. Johnson, M. Zemba, B. P. Conner, J. Walker, E. Burden, K. Rogers, K. R. Cwiok, E. Macdonald, and P. Cortes, "Digital manufacturing of pathologically-complex 3D printed antennas," *IEEE Access*, vol. 7, pp. 39378–39389, 2019.

[6] R. Colella, F. P. Chietera, L. Catarinucci, J. F. Salmeron, A. Rivadeneyra, M. A. Carvajal, A. J. Palma, and L. F. Capitan-Vallvey, "Fully 3D-printed RFID tags based on printable metallic filament: Performance comparison with other fabrication techniques," in *Proc. IEEE-APS Topical Conf. Antennas Propag. Wireless Commun. (APWC)*, Granada, Spain, Sep. 2019, pp. 253–257.

[7] L. Mescia, P. Bia, D. Caratelli, M. A. Chiapperino, O. Stukach, and J. Gielis, "Electromagnetic mathematical modeling of 3D supershaped dielectric lens antennas," *Math. Problems Eng.*, vol. 2016, pp. 1–10, Jan. 2016.

[8] T. Whittaker, S. Zhang, A. Powell, C. J. Stevens, J. Y. C. Vardaxoglou, and W. Whittow, "3D printing materials and techniques for antennas and metamaterials: A survey of the latest advances," *IEEE Antennas Propag. Mag.*, early access, Dec. 26, 2022, doi: 10.1109/MAP.2022.3229298.

[9] F. P. Chietera, R. Colella, A. Verma, E. Ferraris, C. E. Corcione, C. L. Moraila-Martinez, D. Gerardo, Y. H. Acid, A. Rivadeneyra, and L. Catarinucci, "Laser-induced graphene, fused filament fabrication, and aerosol jet printing for realizing conductive elements of UHF RFID antennas," *IEEE J. Radio Freq. Identificat.*, vol. 6, pp. 601–609, 2022.

[10] E. A. Rojas-Nastrucci, J. T. Nussbaum, N. B. Crane, and T. M. Weller, "Ka-band characterization of binder jetting for 3-D printing of metallic rectangular waveguide circuits and antennas," *IEEE Trans. Microw. Theory Techn.*, vol. 65, no. 9, pp. 3099–3108, Sep. 2017.

[11] R. Colella, A. Michel, and L. Catarinucci, "Compact 3-D-printed circularly polarized antenna for handheld UHF RFID readers," *IEEE Antennas Wireless Propag. Lett.*, vol. 17, no. 11, pp. 2021–2025, Nov. 2018.

[12] M. F. Farooqui and A. Kishk, "3-D-printed tunable circularly polarized microstrip patch antenna," *IEEE Antennas Wireless Propag. Lett.*, vol. 18, no. 7, pp. 1429–1432, Jul. 2019.

[13] D. Helena, A. Ramos, T. Varum, and J. N. Matos, "The use of 3D printing technology for manufacturing metal antennas in the 5G/IoT context," *Sensors*, vol. 21, no. 10, p. 3321, May 2021.

[14] I. T. Nassar, T. M. Weller, and H. Tsang, "A 3-D printed miniaturized log-periodic dipole antenna," in *Proc. IEEE Antennas Propag. Soc. Int. Symp. (APSURSI)*, Memphis, TN, USA, Jul. 2014, pp. 6–11.

[15] K. Smith and R. Adams, "A broadband 3D printed fractal tree monopole antenna," *Prog. Electromagn. Res. C*, vol. 86, pp. 17–28, 2018.

[16] S. Alkaraki, A. S. Andy, Y. Gao, K.-F. Tong, Z. Ying, R. Donnan, and C. Parini, "Compact and low-cost 3-D printed antennas metalized using spray-coating technology for 5G mm-wave communication systems," *IEEE Antennas Wireless Propag. Lett.*, vol. 17, no. 11, pp. 2051–2055, Nov. 2018.

[17] S. Alkaraki, Y. Gao, S. Stremsdoerfer, E. Gayets, and C. G. Parini, "3D printed corrugated plate antennas with high aperture efficiency and high gain at X-band and Ka-band," *IEEE Access*, vol. 8, pp. 30643–30654, 2020.

[18] J. Bjorgaard, M. Hoyack, E. Huber, M. Mirzaee, Y.-H. Chang, and S. Noghanian, "Design and fabrication of antennas using 3D printing," *Prog. Electromagn. Res.*, vol. 84, pp. 119–134, 2018.

[19] S. Shrestha, A. A. Baba, S. M. Abbas, M. Asadnia, and R. M. Hashmi, "A horn antenna covered with a 3D-printed metasurface for gain enhancement," *Electronics*, vol. 10, no. 2, p. 119, Jan. 2021.

[20] Y. Li, C. Wang, H. Yuan, N. Liu, H. Zhao, and X. Li, "A 5G MIMO antenna manufactured by 3-D printing method," *IEEE Antennas Wireless Propag. Lett.*, vol. 16, pp. 657–660, 2017.

[21] M. Mirmozafari, S. Saeedi, H. Saeidi-Manesh, G. Zhang, and H. H. Sigmarsson, "Direct 3-D printing of nonplanar linear-dipole-phased array antennas," *IEEE Antennas Wireless Propag. Lett.*, vol. 17, no. 11, pp. 2137–2140, Nov. 2018.

[22] J. Teniente, J. C. Iriarte, R. Caballero, D. Valcazar, M. Goni, and A. Martinez, "3-D printed horn antennas and components performance for space and telecommunications," *IEEE Antennas Wireless Propag. Lett.*, vol. 17, no. 11, pp. 2070–2074, Nov. 2018.

[23] C. Gu, S. Gao, V. Fusco, G. Gibbons, B. Sanz-Izquierdo, A. Standaert, P. Reynaert, W. Bösch, M. Gadringer, R. Xu, and X. Yang, "A D-band 3D-printed antenna," *IEEE Trans. THz Sci. Technol.*, vol. 5, no. 12, pp. 433–442, Sep. 2020.

[24] J. Olivová, M. Popela, M. Richterová, and E. Štefl, "Use of 3D printing for horn antenna manufacturing," *Electronics*, vol. 11, no. 10, p. 1539, May 2022.

[25] F. Pizarro, R. Salazar, E. Rajo-Iglesias, M. Rodríguez, S. Fingerhuth, and G. Hermosilla, "Parametric study of 3D additive printing parameters using conductive filaments on microwave topologies," *IEEE Access*, vol. 7, pp. 106814–106823, 2019.
[26] D. Mitra, S. Roy, R. Striker, E. Burczek, A. Aqueeb, H. Wolf, K. S. Kabir, S. Ye, and B. D. Braaten, "Conductive electrifi and nonconductive NinjaFlex filaments based flexible microstrip antenna for changing conformal surface applications," *Electronics*, vol. 10, no. 7, p. 821, Mar. 2021.
[27] *BlackMagic3D*. Accessed: Aug. 1, 2020. [Online]. Available: http://www.blackmagic3d.com/Conductive-p/grphn-pla.htm Last
[28] *Proto-Pasta*. Accessed: Aug. 1, 2020. [Online]. Available: https://www.proto-pasta.com/pages/conductive-pla
[29] *FiberForce*. Accessed: Aug. 1, 2020. [Online]. Available: http://www.fiberforce.it/products-pro/
[30] *Multi3D*. Accessed: Aug. 1, 2020. [Online]. Available: https://www.multi3dllc.com/
[31] S. Roy, M. B. Qureshi, S. Asif, and B. D. Braaten, "A model for 3D-printed microstrip transmission lines using conductive electrifi filament," in *Proc. IEEE Int. Symp. Antennas Propag. USNC/URSI Nat. Radio Sci. Meeting*, San Diego, CA, USA, Jul. 2017, pp. 1099–1100.
[32] O. Yurduseven, P. Flowers, S. Ye, D. L. Marks, J. N. Gollub, T. Fromenteze, B. J. Wiley, and D. R. Smith, "Computational microwave imaging using 3D printed conductive polymer frequency-diverse metasurface antennas," *IET Microw., Antennas Propag.*, vol. 11, no. 14, pp. 1962–1969, Nov. 2017.
[33] R. Colella, F. P. Chietera, A. Michel, G. Muntoni, G. Casula, G. Montisci, and L. Catarinucci, "Electromagnetic characterisation of conductive 3D-printable filaments for designing fully 3D-printed antennas," *IET Microw., Antennas Propag.*, vol. 16, no. 11, pp. 687–698, Sep. 2022.
[34] G. Muntoni, G. Montisci, G. A. Casula, F. P. Chietera, A. Michel, R. Colella, L. Catarinucci, and G. Mazzarella, "A curved 3-D printed microstrip patch antenna layout for bandwidth enhancement and size reduction," *IEEE Antennas Wireless Propag. Lett.*, vol. 19, no. 7, pp. 1118–1122, Jul. 2020.
[35] G. Muntoni, G. Montisci, A. Melis, M. B. Lodi, N. Curreli, M. Simone, G. Tedeschi, A. Fanti, T. Pisanu, I. Kriegel, A. Athanassiou, and G. Mazzarella, "A curved 3D-printed S-Band patch antenna for plastic CubeSat," *IEEE Open J. Antennas Propag.*, vol. 3, pp. 1351–1363, 2022.
[36] *Qualcomm*. Accessed: Dec. 1, 2022. [Online]. Available: https://www.qualcomm.com/media/documents/files/spectrum-for-4g-and-5g.pdf
[37] D. M. Pozar, *Microwave Engineering*. Hoboken, NJ, USA: Wiley, 2011.
[38] C. A. Balanis, *Antenna Theory: Analysis and Design*. Hoboken, NJ, USA: Wiley, 2005.

RICCARDO COLELLA (Senior Member, IEEE) received the M.Sc. degree (Hons.) in telecommunication engineering and the Ph.D. degree from the University of Salento, Italy, in 2010 and 2015, respectively. He is currently a Researcher of electromagnetic fields area with the Department of Innovation Engineering, University of Salento. He has authored about 150 papers that appeared in international journals and at national and international conferences, two book chapters with international diffusion, and a patent. His research interests include the design of innovative RFID antennas, wirelessly powered IoT sensing systems, antennas for healthcare applications, and novel RF electronic devices and antennas in 3D-printing technology.

FRANCESCO P. CHIETERA (Student Member, IEEE) received the M.S. degree in communication engineering from the University of Salento, Lecce, Italy, in 2018, with a thesis named "Enhanced UHF RFID Antennas exploiting Additive Manufacturing 3D printing." He is currently pursuing the Ph.D. degree with the Department of Innovation Engineering and the Electromagnetic Solutions for Hi-Tech (EMTech) Group, University of Salento, under the supervision of Prof. Luca Catarinucci. His research interests include 3D printing in electromagnetics, with a particular focus on RFID technologies for sensing and traceability and the IoT applications, in general. He coauthored more than 30 papers on these topics both in international journals and conferences.

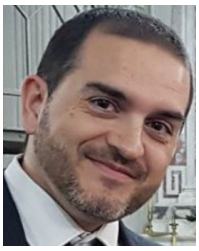

GIACOMO MUNTONI received the bachelor's degree in electronic engineering, the master's degree in telecommunication engineering, and the Ph.D. degree in electronic engineering and computer science from the University of Cagliari, in 2010, 2015, and 2019, respectively.

He is currently a Technologist with the Applied Electromagnetics Group, University of Cagliari. His research interests include the design and characterization of antennas for biomedical and aerospace applications, microwave-based dielectric characterization of materials, 3D printing of RF components, and monitoring of the space debris environment in low-Earth orbit with Sardinia Radio Telescope, in collaboration with Cagliari Astronomical Observatory.

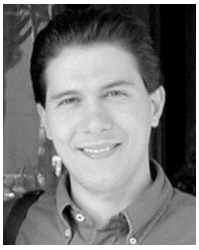

GIOVANNI A. CASULA (Senior Member, IEEE) received the M.S. degree in electronic engineering and the Ph.D. degree in electronic engineering and computer science from the University of Cagliari, Cagliari, Italy, in 2000 and 2004, respectively.

Since December 2017, he has been an Associate Professor of electromagnetic fields with the University of Cagliari, teaching courses in electromagnetics and antenna engineering. He has authored or coauthored about 50 articles in international journals. His current research interests include the analysis and design of waveguide slot arrays, RFID antennas, wearable antennas, and numerical methods in electromagnetics. He is an associate editor of IEEE TRANSACTIONS ON ANTENNAS AND PROPAGATION, *IET Microwaves, Antennas and Propagation*, *Electronics* (MDPI), and *Sensors* (MDPI), and an Academic Editor of the *International Journal of Antennas and Propagation*.

GIORGIO MONTISCI (Senior Member, IEEE) received the M.S. degree in electronic engineering and the Ph.D. degree in electronic engineering and computer science from the University of Cagliari, Cagliari, Italy, in 1997 and 2000, respectively. Since February 2022, he has been a Full Professor of electromagnetic fields with the University of Cagliari, teaching courses in electromagnetics and microwave engineering. He has authored or coauthored 80 articles in international journals. His current research interests include the analysis and design of waveguide slot arrays, RFID antennas, wearable antennas, numerical methods in electromagnetics, and microwave circuits and systems. He was awarded IEEE ACCESS Outstanding Associate Editor of 2020 and 2021. He is an Associate Editor of IEEE ACCESS, *IET Microwaves, Antennas and Propagation*, and *IET Electronics Letters*, and an Academic Editor of the *International Journal of Antennas and Propagation*.

LUCA CATARINUCCI (Senior Member, IEEE) is currently an Associate Professor of electromagnetic fields with the Department of Innovation Engineering, University of Salento, Lecce, Italy, where he teaches microwaves and electromagnetic solutions for HiTech. Besides various activities in the classical areas of electromagnetics, in 2005, he began a new research tread referred to radiofrequency identification systems (RFID), dealing with reader and tag antenna design, the realization of microwave circuits for the integration of UHF RFID systems with sensor networks, the design of automatic platforms for the over-the-air performance evaluation of RFID tags, the prototyping of fully passive RFID tags provided with computational and sensing capabilities, the study of new antennas for handheld RFID readers, the joint use of 3D-printed electronics and RFIDs, and the introduction of Doppler-based RFID-inspired backscattering modulation. He is currently the Vice President of Technical Activities with the IEEE Council of RFID (CRFID). He has authored more than 200 scientific works of which 83 on international journals, four chapters of books with international diffusion, and more than 89 proceedings at international conferences. Moreover, he holds two national patents for RFID technology.

Open Access funding provided by 'Università degli Studi di Cagliari' within the CRUI CARE Agreement